Journal of Fluorine Chemistry 173 (2015) 77–83

Contents lists available at ScienceDirect

Journal of Fluorine Chemistry

journal homepage: www.elsevier.com/locate/fluor

Synthesis, Ni(II) Schiff base complexation and structural analysis of fluorinated analogs of the ligand (*S*)-2-[*N*-(*N*′-benzylprolyl)amino]benzophenone (BPB)

Natalie J. Tatum [b], Dmitry S. Yufit [b], Steven L. Cobb [b,*], Christopher R. Coxon [a,*]

[a] School of Pharmacy and Biomolecular Sciences, Byrom Street Campus, Liverpool John Moores University, Liverpool L3 3AF, UK
[b] Department of Chemistry, Durham University, South Road, Durham DH1 3LE, UK

ARTICLE INFO

Article history:
Received 23 October 2014
Received in revised form 30 January 2015
Accepted 12 February 2015
Available online 25 February 2015

Keywords:
Fluoro-proline
Fluorinated ligands
Gauche effect
Nickel complex
X-ray crystallography

ABSTRACT

Herein we report the first X-ray crystal structure of the well-known (*S*)-L-ala-Ni-BPB complex (**1**) and compare this with the X-ray crystal structures obtained for two novel fluorinated (*S*)-L-ala-Ni-BPB complexes (**8** and **12**) that contain either an *S*- or *R*-fluorine atom on the proline ring of the BPB ligand. The preparation of complexes **8** and **12** has been enabled by the synthesis of two new fluorinated BPB ligands (**7** and **11**). In this work we looked to observe the structural effects that the introduction of a single fluorine atom had on the known complex **1**. Arising from this, we highlight a novel fluorine–nickel interaction that on the basis of DFT calculations appears to provide additional stabilization to one of the complexes prepared ((*S*)-L-ala-Ni-BPB complex **8**).

1. Introduction

The introduction of a fluorine atom in to a molecule can have a remarkable effect on its physical and chemical properties, metabolic stability and its biological activity. This has been widely exploited within medicinal chemistry and is discussed in detail in a number of recent review articles [1]. Fluorine substitution can also be used to fine-tune the stereo-electronic properties of a molecule and in doing so allow conformational control [2,3]. For example β-fluoro imines have been shown by X-ray crystallographic analysis and theoretical DFT calculations, to have a torsion angle (Φ) of approximately 60° about the NCCF bonds (Fig. 1), therefore, preferentially adopting a *gauche* conformation [4]. This is explained by first, the avoidance of an electronically destabilising *anti*-arrangement around the NCCF bond (Fig. 1), in which the electron-withdrawing fluorine atom lies directly opposite to the electron deficient imine or ammonium group. Second, the favoured conformation puts a hydrogen atom *anti*- to the imminium or ammonium group, thus allowing a stabilising electron-donation from σ_{C-H} to $\sigma^*_{C-N^+}$ by hyperconjugation (Fig. 1). This has been utilised as a tool in medicinal chemistry, where introduction of a single fluorine atom with the correct stereochemistry selectively stabilises a compound in a biologically active conformation e.g. 3-fluoro-*N*-methyl-D-aspartic acid, whereas, the opposite enantiomer stabilises an inactive conformer [5]. Furthermore, 4-fluoroprolines have been incorporated in to collagen triple helices with the observation that this modification confers hyperstability within these structures due to the above stereoelectronic effects [6]. A similar approach using fluoropyrrolidine derivatives (Fig. 1) has also been pioneered recently by the Gilmour group as a method to control molecular conformation in acyclic systems, and thus, probe catalyst mechanism, reactivity and selectivity in asymmetric organocatalysis [7].

Nickel(II) Schiff base complexes of (*S*)-2-[*N*-(*N*′-benzylprolyl)amino]benzophenone (BPB) and amino acids (e.g. **1**) have been widely used as nucleophilic glycine equivalents in the asymmetric synthesis of C_α-substituted amino acids [8]. Soloshonok et al. have also investigated the modification of the chelating ligand, replacing the proline ring in **1** to prepare novel NH–Ni ligands and observing the resulting disatereomeric ratio of the Ni-complexes and the consequences in alkylation and Michael addition reactions [9,10]. Incorporation of fluorine at the 3-position of protonated pyrrolidines has been shown to stabilise particular conformations through β-fluoro-ammonium interactions [11]. In light of this we hypothesised that incorporation of a single fluorine atom on the proline ring within the BPB ligand could offer a novel route to modulate the

* Corresponding authors at: Durham University, Department of Chemistry, South Road, Durham DH1 3LE, United Kingdom and School of Pharmacy and Biomolecular Sciences, Byrom Street Campus, Liverpool John Moores University, Liverpool L3 3AF, United Kingdom. Tel.: +44 191 334 2086; fax: +44 191 384 4737.
E-mail addresses: s.l.cobb@durham.ac.uk (S.L. Cobb), c.r.coxon@ljmu.ac.uk (C.R. Coxon).

http://dx.doi.org/10.1016/j.jfluchem.2015.02.007

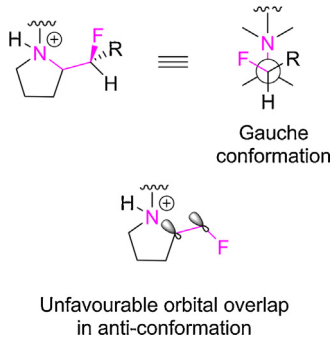

Fig. 1. Fluorine-ammonium *gauche* effect in 5-membered nitrogen-containing heterocycles [6].

conformation and hence the reactivity of a BPB-nickel(II) type complex. As such, we sought to probe whether the introduction of a fluorine atom in the correct configuration at the carbon beta to the proline nitrogen atom in **1** could invoke conformational effects, such as a fluorine-ammonium ion *gauche* effect, leading to complexes with an altered chelate ring configuration around the nickel atom.

Here we report the synthesis and the first ever X-ray crystal structure of the well-known (*S*)-L-Ala-Ni-BPB Schiff base complex (**1**). This structure has been compared with the X-ray crystal structures obtained for two novel fluorinated (*S*)-L-Ala-Ni-BPB complexes (**8** and **12**) that contain either an *S*- or *R*-fluorine atom on the proline ring of the BPB ligand. The preparation of complexes **8** and **12** has been enabled by the synthesis of two new fluorinated BPB ligands (**7** and **11**). Furthermore, we highlight a novel Ni–F interaction and use DFT calculations to support a role for this in stabilizing one of the nickel complexes prepared.

2. Results and discussion

We initially prepared the reported (*S*)-BPB ligand [12] and corresponding (*S*)-L-Ala-Ni-BPB complex (**1**) [13] according to the published methods and obtained crystals of **1** by slow evaporation from acetone and methylethylketone. This was to provide a comparison of the overall structure of **1** with the fluorinated derivatives in X-ray diffraction studies (Fig. 2). In spite of being synthesized and used many times by researchers in the field of peptide chemistry [14], the structure of complex (**1**) has not yet been reported in the literature (CCDC ver. 5.35 2013). Herein, we report the first X-ray structure of (*S*)-L-Ala-Ni-complex (**1**) (in form of MEK solvate).

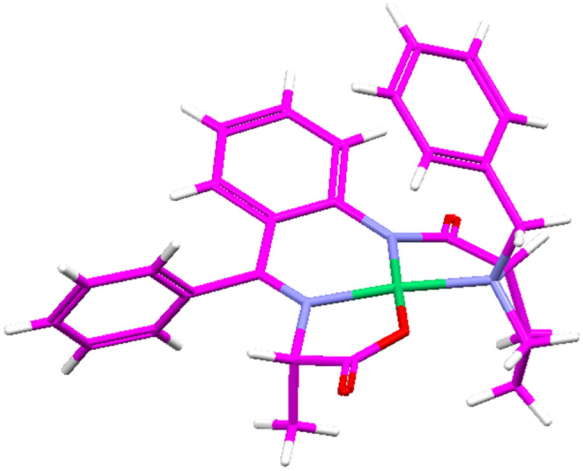

Fig. 2. First reported X-ray crystal structure of (*S*)-L-Ala-Ni-BPB complex **1**. The MEK solvent molecule and one of the component of disordered benzyl group are omitted for clarity. All crystal structure drawings were produced with Olex2 [15]. All structural images produced in Hermes [16].

We attempted to prepare the analogous *R*- and *S*-fluorinated nickel(II) complexes of the L-Schiff base of (*S*)-2-[*N*-(*N*′-benzylprolyl)amino]benzophenone (BPB) and L-alanine (**7** and **12**) starting from commercially available proline derivatives (Schemes 1 and 2, respectively). *trans*-Hydroxyproline methyl ester (*trans*-HypOMe, **2**) was protected as the reported [17] *N*-(*tert*-butylcarbamate) (**3**) prior to a 2-step fluorination procedure employing tetrabutylammonium difluorotriphenylsilicate (TBAT) followed by treatment with perfluoro-1-butanesulfonyl fluoride (PBSF), with inversion of stereochemistry at the 4-position [18]. Removal of the Boc protecting group preceded *N*-benzylation using standard conditions. Conversion of the methyl ester (**6**) in to the required amide (**7**) was achieved directly through an oxidative process involving potassium *tert*-butoxide and exposure to atmospheric oxygen [19].

To prepare the alternative (*R*)-fluorinated ligand (Scheme 2), commercially sourced *N*-Boc-*trans*-4-fluoro-L-proline (**9**) was deprotected by treatment with trifluoroacetic acid and used directly in an *N*-benzylation reaction without purification (Scheme 2) [20]. On this occasion, the free acid of **10** was coupled with 2-aminobenzophenone to afford amide **11** by initial conversion of the acid in to a mixed anhydride intermediate [21].

With the fluorinated BPB ligands (**7** and **11**) in hand, we subsequently attempted to prepare the corresponding Ni-complexes (Scheme 3). Following the standard protocol for complexation with Ni(II), chiral ligand **7** was treated with nickel(II) nitrate hexahydrate and L-alanine under basic conditions with gentle heating. This reaction was performed in parallel with the analogous reaction to prepare the reported des-fluoro complex **1**. After 2 h formation of **1** was complete and afforded a deep red solution. By comparison, more than 72 h were required for the (*S*)-fluorinated derivative (**8**) to reach completion. *R*-fluoro-BPB ligand **11**, however, formed the desired Ni(II) complex (**12**) rapidly, within 20 min according to TLC, however, heating was continued for 24 h to ensure complete conversion. Crystals of complexes **8** and **12** were obtained as dark red needles by slow evaporation from diethyl ether and the structures were determined by X-ray analysis.

It was proposed that, with the correct (*S*)-stereochemistry at the fluorine position, we would be able to stabilise the existing conformation by replacement of a hydrogen atom already orientated in the *gauche* conformation with respect to the nearby nickel-coordinating nitrogen atom (Fig. 2).

The fluorinated and non-fluorinated complexes were aligned using the central nickel and its coordinated heteroatoms in molecular viewer Hermes [16] to an RMSD of less than 0.01 Å (Fig. 3). The structure **8** contained two independent molecules with virtually identical configuration of the coordination polyhedron of metal atom. Overlay of **1** and **8** (Fig. 4) showed that replacement of the corresponding *gauche* hydrogen with fluorine does not perturb the favoured conformation with respect to the benzyl group. We observed that the fluorine atom of **8** lies in the anticipated *gauche* conformation (Fig. 5), with a measured NCCF bond torsion angle of 76° (slightly greater than 60° due to ring strain in the pyrrolidine) that is consistent with the corresponding non-fluorinated complex (**1**).

Replacement of the hydrogen atom with fluorine introduces two further interesting intramolecular features in **8**. First, a putative intramolecular C–H···F bond may be observed (Fig. 5). The existence of such interactions is controversial and many authors have concluded that any interaction may be only providing van der Waals stabilisation [22]. However, others have reported

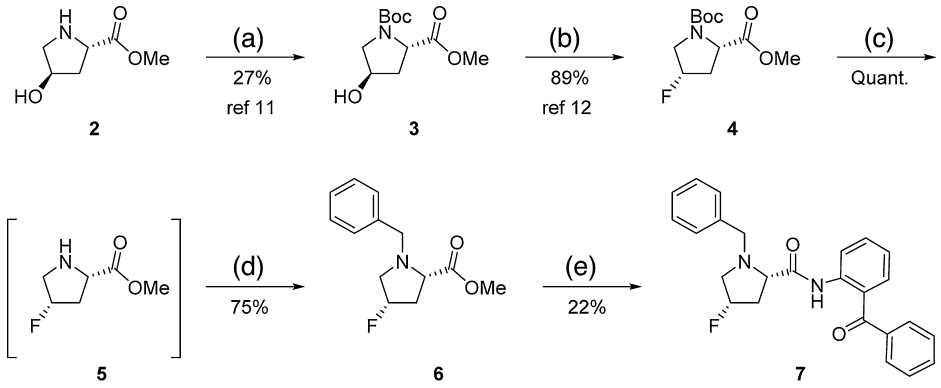

Scheme 1. Reagents and conditions: (a) Boc_2O, NEt_3, CH_2Cl_2, rt, 18 h; (b) (i) TBAT, DIPEA, CH_2Cl_2, (ii) PBSF, rt, 72 h; (c) TFA, CH_2Cl_2, rt, 2 h (used in next step without purification); (d) benzyl bromide, K_2CO_3, DMF, rt, 20 h; (e) 3-aminobenzophenone, ^tBuOK, THF, open to air, rt, 70 min.

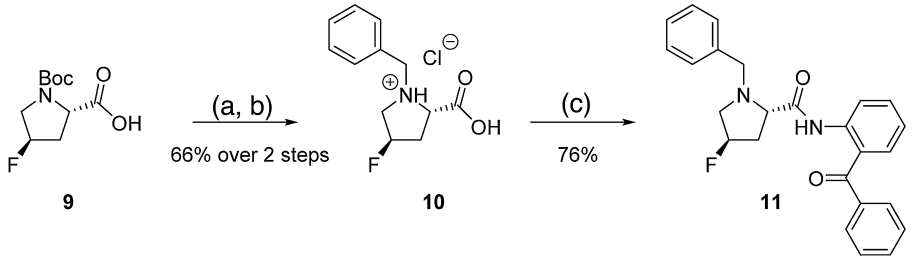

Scheme 2. Reagents and conditions: (a) TFA, CH_2Cl_2, rt, 2 h (used in next step without purification); (b) benzyl chloride, KOH, ^iPrOH, 50 °C, 6 h; (c) MsCl, 2-aminobenzophenone, Et_3N, CH_2Cl_2.

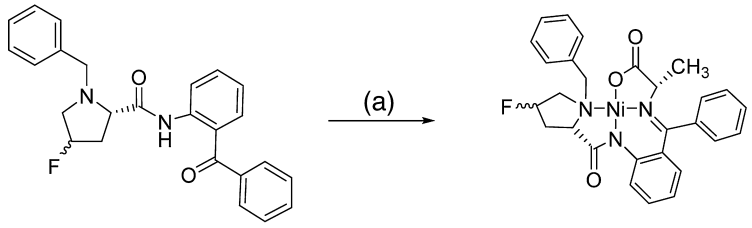

7: X = (*S*)-Fluoro-BPB
11: X = (*R*)-Fluoro-BPB

8: X = (*S*)-L-Ala-Ni-(*S*)-Fluoro-BPB (55%)
12: X = (*S*)-L-Ala-Ni-(*R*)-Fluoro-BPB (71%)

Scheme 3. Reagents and conditions: (a) L-alanine, $Ni(NO_3)_2{\cdot}6H_2O$, MeOH, KOH, 60 °C, 24–72 h.

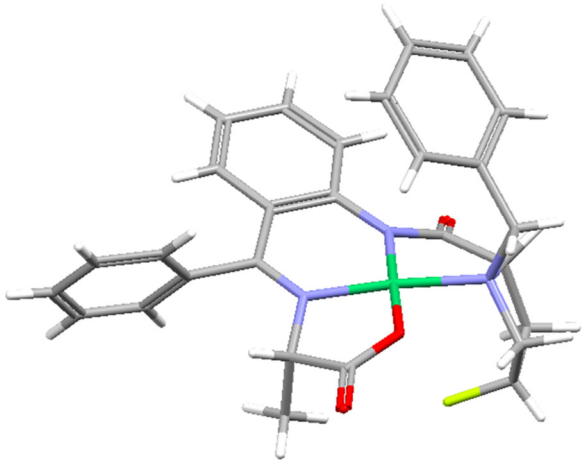

Fig. 3. X-ray crystal structure of L-Ala-Ni-(*S*)-FBPB complex **8**.

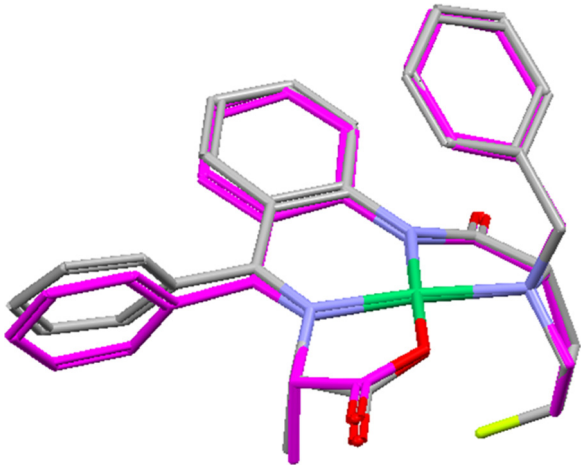

Fig. 4. Least-squares superposition of fluorinated complex **8** (grey) with non-fluorinated complex **1** (pink). (For interpretation of the references to color in this figure legend, the reader is referred to the web version of this article.)

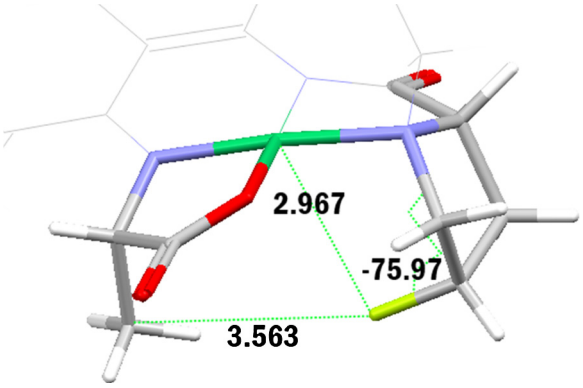

Fig. 5. Expansion of a section of complex **8** showing the measured NCCF bond torsion angle of 76° and also displaying a putative C–H···F bond.

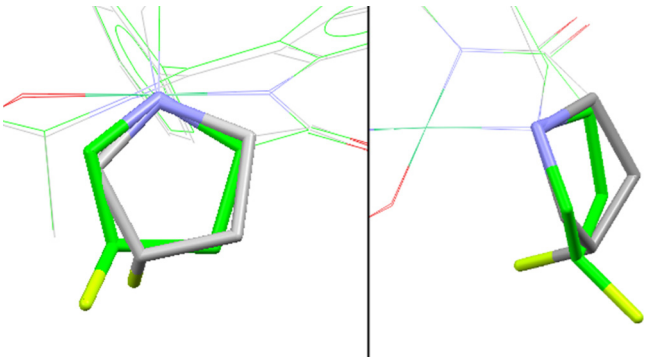

Fig. 7. The proline ring of complex **12** (green) is twisted, whereas the ring of complex **8** (grey) adopts an envelope conformation. (For interpretation of the references to color in this figure legend, the reader is referred to the web version of this article.)

that despite being very weak non-covalent interactions, C–H···F interactions have been observed in organic structures, notably in some fluorobenzenes [23], and that these may be enhanced when the proton of the C–H bond is more acidic [24]. In complex **8** the fluorine atom is found to be within hydrogen bonding distance (2.64 Å) of the proximal methyl hydrogens (Fig. 5). Although these are likely to be weak interactions, this could confer additional stability to the molecule. Second, as observed in the crystal structure, fluorine is positioned directly below the central nickel ion at a distance of 2.97 Å, which is smaller than the sum of their van der Waals radii (3.10 Å). As no alteration in the crystal structure of **8** is observed relative to the non-fluorinated compound **1** (Fig. 4) e.g. due to repulsion between the F and Ni atoms, this may suggest that a non-bonding interaction arises, which may stabilise the complex.

Complex **12** was aligned to complex **1** as described above, to an RMSD of 0.05 Å. The greatest difference in the structures, as seen in Fig. 6, is in the fluorinated proline ring. The position of the fluorine in complex **12** abolishes the potential nickel interaction observed in complex **8**. Furthermore, the proline ring in complex **12** is twisted, where it is in the envelope conformation in complex **8** (Fig. 7). A comparison of complex **12** with the CSD (version 5.35) using Mogul shows the torsions within this ring to be well represented, with the nearest comparable structure only 0.89° RMSD difference over ring torsions, and with 40% of the returned structures within 10°. Finally, the NCCF torsion angle of complex **12** differs greatly from that of complex **8** (Table 1, Fig. 8), which is an expected change resulting from introduction of equatorial and axial substituents.

To investigate the differences between the complexes in more detail DFT, calculations were carried out using the crystal structures of complexes **8** and **12**. By comparing the calculated energies of the *R*-fluorine and *S*-fluorine complexes it would be possible to estimate the strength of the interaction between *S*-fluorine and nickel. DFT calculations were performed as implemented in the Gaussian03 package. The B3LYP functional was used in conjunction with the 6-311 + +G** basis set. The difference in calculated energies between the two complexes (**8** and **12**) was determined to be 5.99 kJ/mol (in favour of the *S*-fluorine complex **8**). This energy difference supports the notion of a stabilizing non-bonding interaction between the *S*-fluorine and the nickel in complex **8** as observed in the X-ray structure.

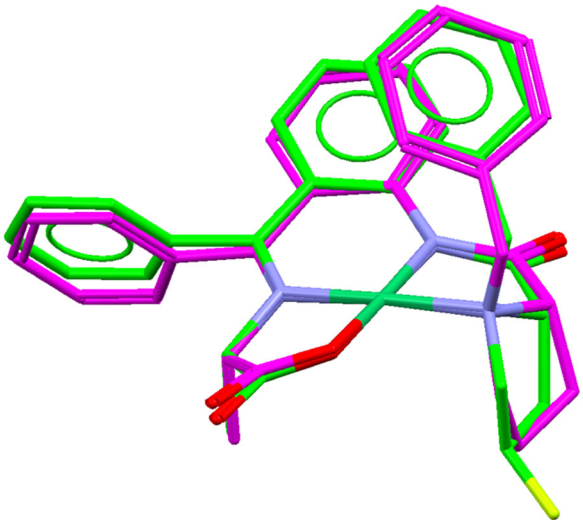

Fig. 6. Least squares superposition of complex **1** (pink) and complex **12** (green). (For interpretation of the references to color in this figure legend, the reader is referred to the web version of this article.)

Table 1
Torsion angles for ΦNCCH and ΦNCCF. * For complex **1**, $NCCH_2$ angle is given as NCCF for comparison.

Ni complex	ΦNCCH (°)	ΦNCCF (°)
1	−73.31	161.70*
8	162.98	−75.97
12	−86.23	152.36

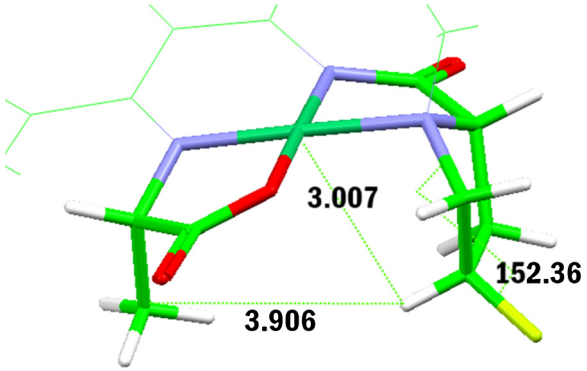

Fig. 8. The NCCF torsion angle of complex **12** is 152.4°.

3. Conclusions

Here we report the first X-ray crystal structure of the known nickel(II) Schiff base complex (**1**). This structure has been compared with the X-ray crystal structures obtained for two novel fluorinated nickel(II) Schiff base complexes that contain either an *S*- and *R*-fluorine atom beta to the proline nitrogen on the BPB ligands (**8** and **12**, respectively). We discovered that the introduction of an *S*-fluorine atom (complex **8**) has no significant effect upon the overall structural geometry of the complex. However, whilst we accept that these may be artifacts of the structures being solved in the crystal form, we speculate that inclusion of a *S*-fluorine atom may enhance the stability of complex **8** through a combination of the formation of a C–H···F bond and a novel Ni···F non-bonding interaction. DFT calculations support this hypothesis, with a clear difference in the calculated energies of 5.99 kJ/mol between the *S*-fluorinated complex **8** and the *R*-fluorinated complex **12** (no Ni···F interaction observed in the X-ray structure). Introduction of the *R*-fluorine atom substituent (complex **12**) also afforded no significant overall changes to the structure although as expected some minor conformational changes in the proline ring of complex **12** were observed. Further investigations to probe any differences between complex **1** and the fluorinated complexes **8** and **12**, with regard to reactivity and stability, are currently underway.

4. Experimental

4.1. Materials

L-4-*trans*-Hydroxyproline methyl ester hydrochloride (**2**) (Novabiochem) and *N*-Boc-*cis*-4-fluoro-L-proline methyl ester (**9**) (Sigma Aldrich) were purchased from commercial suppliers and used directly as indicated in the appropriate experimental procedures. All other chemicals were purchased from Sigma Aldrich. Complex **1** [10] and intermediates **3** [12] and **4** [13] were prepared according to literature procedures and the obtained analytical data was in accordance with the published characterizations. The preparation of *N*-benzyl-(*S*)-4-fluoro-L-proline methyl ester (**6**) followed a previously undescribed route (details below) but analysis indicated that this was identical to the reported substance [19].

4.2. Characterization

NMR spectra were collected using Bruker Avance 400 MHz or Varian VNMRS 700 MHz spectrometers. Multiplicities are reported as: s = singlet, d = doublet, m = multiplet, t = triplet or combinations thereof e.g. dd = doublet of doublets. Chemical shifts are reported in ppm and are referenced to residual solvent peaks; $CHCl_3$ (^{1}H 7.26 ppm, ^{13}C 77.2 ppm), H_2O (^{1}H 4.79 ppm). *J* couplings are measured in Hertz (Hz). Reactions were monitored by TLC using Merck precoated silica gel plates. Column chromatography was performed using silica gel with the solvent system indicated. All reported yields refer to the isolated yield and the product purity was estimated to be >95% by ^{1}H NMR. IR spectra were recorded on a Perkin Elmer Spectrum RX1 fitted with an ATR attachment. IR absorptions reported are in cm^{-1}. Mass spectra were collected on a Waters TQD mass spectrometer and accurate mass spectra were collected on a Waters LCT Premier XE mass spectrometer. Optical rotations were measured using a Jasco P-1020 polarimeter with samples in the solvents, temperatures and concentrations as indicated.

4.2.1. N-*Benzyl-(S)-4-fluoro-L-proline methyl ester* (**6**) [19]

A solution of **4** (0.50 g, 2.00 mmol) in CH_2Cl_2 (25 mL) and trifluoroacetic acid (2.5 mL) was stirred at room temperature for 2 h. Upon completion of the reaction, volatiles were removed under reduced pressure, affording a colourless solid (0.29 g, quant.). Trifluoroacetate salt **5** was used directly in the subsequent step without further purification. Potassium carbonate (1.47 g, 10.6 mmol) was added to a rapidly stirred suspension of **5** (0.55 g, 2.12 mmol) in anhydrous DMF (50 mL) and gradually reached homogeneity after 1 h at room temperature. Benzyl bromide was added in one portion and the reaction mixture was stirred for a further 48 h at room temperature until TLC indicated the complete consumption of starting materials. The crude mixture was poured over crushed ice and stirred until thawing was complete and the emulsion was extracted with Et_2O (100 mL), which was then washed with brine (sat.) (3 × 30 mL). Purification by column chromatography (silica; EtOAc—hexane 0% to 50%) afforded the desired product (0.39 g, 75%). All analyses were consistent with the reported preparation [25].

Pale yellow oil, ^{1}H NMR (400 MHz, $CDCl_3$): δ 7.35–7.22 (m, 5*H*, Ph), 5.08 (dm, *J* = 54.7 Hz, 1*H*, CHF), 4.02 (d, *J* = 13.1 Hz, 1*H*, benzyl CH), 3.69 (s, 3*H*, OMe), 3.58 (d, *J* = 13.1 Hz, 1*H*, benzyl CH), 3.33–3.20 (m, 2*H*, CH_2), 2.63–2.42 (m, 2*H*, CH_2), 2.27 (m, 1*H*, CH); ^{13}C NMR (101 MHz, $CDCl_3$): δ 172.2, 136.4, 128.1, 127.3, 126.3, 91.0 (d, J_{C-F} = 173.2 Hz), 62.7, 58.2 (d, J_{C-F} = 22.1 Hz), 56.8, 51.0, 36.2 (d, J_{C-F} = 22.1 Hz); ^{19}F NMR (376 MHz, $CDCl_3$): δ −168.99 (m, 1*F*); LCMS (ESI+) 238.09 $[M+H]^+$.

4.2.2. (*S*)-2-[N-(N′-*benzyl-(S)-4-fluoro-L-prolyl)amino]benzophenone* (**7**)

The methyl ester **6** (0.26 g, 1.1 mmol) was added to a solution of ^{t}BuOK (0.25 g, 2.19 mmol) in moist THF (15 mL), which was pre-stirred open to the air for 1 min. Addition of 2-aminobenzophenone (0.22 g, 1.1 mmol). After stirring at room temperature for 1 h TLC indicated that the reaction was incomplete. Additional ^{t}BuOK (123 mg, 1.1 mmol) was added and again stirred for 1 h. The crude mixture was concentrated in vacuo and partitioned between CH_2Cl_2 (20 mL) and water (20 mL). The organic extract was dried ($MgSO_4$) and concentrated to an oil. The title compound was isolated after column chromatography (silica; EtOAc—hexane 0% to 30%) (97 mg, 22%) as a pale yellow oil.

$[\alpha]_D^{23}$ 41.1 (*c* = 1.0, $CHCl_3$); ^{1}H NMR (400 MHz, $CDCl_3$): δ 11.61 (s, 1*H*, NH), 8.55 (d, *J* = 8.3 Hz, 1*H*, Ar), 7.83–7.75 (m, 2*H*, Ar), 7.62–7.56 (m, 1*H*, Ar), 7.56–7.45 (m, 4*H*, Ar), 7.45–7.38 (m, 2*H*, Ar), 7.22–7.15 (m, 3*H*, Ar), 7.09 (t, *J* = 7.6 Hz, 1*H*, Ar), 5.10 (dt, *J* = 52.9, 4.1 Hz, 1*H*, CHF), 4.00 (d, *J* = 13.0 Hz, 1*H*, benzyl CH), 3.63 (d, *J* = 13.0 Hz, 1*H*, benzyl CH), 3.55–3.39 (m, 2*H*, CH), 2.70–2.43 (m, 2*H*, CH_2), 2.31 (m, 1*H*, CFCH), 1.26 (s, 1*H*, CH); ^{13}C NMR (101 MHz, $CDCl_3$): δ 199.1, 172.2, 139.7, 139.0, 137.6, 133.5, 132.7, 128.3, 127.5, 127.3, 126.2, 125.2, 121.7, 120.9, 92.2 (d, J_{C-F} = 179.5 Hz), 62.4, 58.4 (d, J_{C-F} = 22.0 Hz), 57.0, 51.1, 36.6 (d, J_{C-F} = 22.1 Hz); ^{19}F NMR (376 MHz, $CDCl_3$): δ −172.11 (m, 1*F*); IR (neat) υ 3320, 2945, 1675, 1655, 1287, 1115, 703 cm^{-1}; LCMS (ESI+) *m*/*z* = 403.19 $[M+H]^+$. HRMS (ESI) calcd for $C_{25}H_{24}FN_2O_2$ $[M+H]^+$: *m*/*z* = 403.1812, found 403.1822.

4.2.3. L-*Ala-Ni-(S)-fluoro-BPB complex* (**8**)

To a solution of **7** (27 mg, 0.08 mmol) and $Ni(NO_3)_2{\cdot}6H_2O$ (44 mg, 0.15 mmol) in anhydrous methanol (2 mL) was added a solution of KOH (34 mg, 0.60 mmol) and L-alanine (34 mg, 0.38 mmol) in methanol (1 mL). This mixture was heated at 60 °C with stirring for 72 h—TLC indicated the reaction was complete and the deep red solution concentrated in vacuo before partitioning between water (30 mL) and $CHCl_3$ (20 mL). Trituration of the concentrated organic extract under Et_2O afforded a dark red solid that was isolated by filtration under suction and washed with more Et_2O. Purification of the crude material by preparative TLC (silica; acetone—$CHCl_3$ 20%) afforded a red/orange solid (22 mg, 55%).

mp 288–290 °C (dec.); $[\alpha]_D^{27} + 255$ (c = 2.0, $CHCl_3$); ^{1}H NMR (700 MHz, $CDCl_3$): δ 8.09 (d, J = 7.9 Hz, 3*H*, Ar), 7.54–7.47 (m, 2*H*, Ar), 7.47–7.42 (m, 1*H*, Ar), 7.38 (t, J = 7.7 Hz, 2*H*, Ar), 7.25–7.21 (m, 2*H*, Ar), 7.14 (ddd, J = 8.7, 6.9, 1.8 Hz, 1*H*, Ar), 6.97 (dm, J = 7.7 Hz, 1*H*, Ar), 6.67 (m, 1*H*, Ar), 6.62 (dd, J = 7.7, 1.8 Hz, 1*H*, Ar), 5.49 (dm, J = 52.7 Hz, 1*H*, CHF), 4.59 (d, J = 12.7 Hz, 1*H*, benzyl CH), 3.99 (m, 1*H*, CH), 3.90 (m, 1*H*, CH), 3.65 (dd, J = 11.6, 4.7 Hz, 1*H*, CH), 3.58 (d, J = 12.7 Hz, 1*H*, benzyl CH), 2.91 (m, 1*H*, CH), 2.76 (m, 1*H*, CH), 2.25 (ddd, J = 36.4, 11.6, 3.5 Hz, 1*H*, CH), 1.60 (m, 3*H*, CH_3); ^{13}C NMR (101 MHz, $CDCl_3$): δ 179.9, 170.1, 141.9, 133.4, 133.1, 132.6, 131.9, 131.7, 129.6, 129.2, 129.0, 128.8, 127.5, 127.2, 126.7, 123.8, 120.8, 91.4 (d, J = 179.0 Hz), 68.6, 66.9, 62.9, 61.5 (d, J = 20.4 Hz), 38.4 (d, J = 22.4 Hz), 20.3; ^{19}F NMR (376 MHz, $CDCl_3$): δ −167.18 (m, 1*F*); LCMS (ESI+) m/z = 530.12 $[M + H]^+$; HRMS (ESI) calcd for $C_{28}H_{27}FN_3O_3Ni$ $[M + H]^+$: m/z = 530.1382, found 530.1390.

4.2.4. N-*Benzyl-*(R)*-4-fluoro-*L*-proline hydrochloride salt (**10**)*

A solution of *N*-Boc-(*R*)-4-fluoro-L-proline (0.5 g, 2. 18 mmol) in CH_2Cl_2 (25 mL) and trifluoroacetic acid (2.5 mL) was stirred at room temperature for 2 h. Upon completion of the reaction, volatiles were removed under reduced pressure, affording a colourless solid (0.52 g, quant.). The trifluoroacetate salt was used directly in the subsequent step without further purification. A solution of the salt in isopropanol (5 mL) was added to a fully dissolved solution of potassium hydroxide (0.61 g, 10.9 mmol) in isopropanol (25 mL), followed by dropwise addition of benzyl chloride (350 μL, 3.1 mmol) with stirring at 50 °C for 6 h. The pH was adjusted to around 5 by addition of concentrated hydrochloric acid and extracted with $CHCl_3$ (20 mL). Solids were removed by filtration and washed with $CHCl_3$ (2 × 10 mL). The organic extracts were combined and concentrated in vacuo to a pale oil, which was triturated under cold acetone (20 mL) and the resulting analytically pure white solid was isolated by filtration and washed with more cold acetone (10 mL). Additional product was isolated from the acetone washings and was combined with the initial crop (0.37 g, 66%).

mp 213–215 °C; $[\alpha]_D^{27} + 18.9$ (c = 0.95, H_2O); ^{1}H NMR (400 MHz, D_2O): δ 7.49–7.34 (m, 5*H*, Ph), 5.41 (dt, J = 51.7, 3.9 Hz, 1*H*, CHF), 4.54–4.38 (m, 3*H*, CH and benzyl CH_2), 3.98–3.63 (m, 2*H*, CH_2), 2.78 (m, 1*H*, CH), 2.25 (dm, J = 39.3 Hz, 1*H*, CHF); ^{13}C NMR (101 MHz, D_2O): δ 170.7, 130.7, 130.3, 129.3, 91.8 (d, J_{C-F} = 171.7 Hz), 66.5, 60.6, 59.8 (d, J_{C-F} = 21.7 Hz), 36.3 (d, J_{C-F} = 21.7 Hz); ^{19}F NMR (376 MHz, D_2O): δ −173.53 (m, 1*F*); IR (neat) υ 3037, 2944, 1644, 1159 712 cm^{-1}; LCMS (ESI+) 224.28 $[M + H]^+$.

4.2.5. (S)-2-[N-(N′-*benzyl-*(R)*-4-fluoro-*L*-prolyl)amino]benzophenone (**11**)*

Methanesulfonyl chloride (105 μL, 1.36 mmol) was added slowly to a solution containing *N*-methylimidazole (216 μL, 2.72 mmol) and proline acid **10** (0.28 g, 1.24 mmol) in CH_2Cl_2, cooled to 0 °C. After stirring for 10 min, the flask was removed from the ice bath, and 2-aminobenzophenone (0.22 g, 1.12 mmol) was added and the reaction mixture was stirred at 50 °C for 20 h. The reaction was quenched by addition of sat. NH_4Cl aq. (10 mL), the organic phase was extracted CH_2Cl_2 (2 × 20 mL) and volatiles were removed under reduced pressure. The crude mixture was purified by column chromatography (silica; 1:9 ethyl acetate-hexane) and isolated as a pale brown oil (0.38 g, 76%).

$[\alpha]_D^{24}$ 14.1 (c = 1, $CHCl_3$); ^{1}H NMR (400 MHz, $CDCl_3$): δ 11.59 (s, 1*H*, NH), 8.59 (dd, J = 8.4, 1.1 Hz, 1*H*, Ar), 7.81–7.74 (m, 2*H*, Ar), 7.65–7.59 (m, 1*H*, Ar), 7.58–7.47 (m, 4*H*, Ar), 7.46–7.41 (m, 2*H*, Ar), 7.19–7.13 (m, 3*H*, Ar), 7.10 (ddd, J = 8.2, 7.3, 1.1 Hz, 1*H*, Ar), 5.35 (dm, J = 52.0, Hz, 1*H*, CHF), 4.03 (d, J = 13.0 Hz, 1*H*, benzyl CH), 3.78–3.65 (m, 2*H*, CH and benzyl CH), 3.48 (ddd, J = 34.8, 13.1, 4.2 Hz, 1*H*, CH), 2.90 (ddt, J = 28.5, 13.0, 1.8 Hz, 1*H*, CH), 2.72–2.55 (m, 1*H*, CH), 2.22–2.01 (m, 1*H*, CH); ^{13}C NMR (101 MHz, $CDCl_3$): δ 198.3, 172.9, 139.2, 138.5, 137.9, 133.6, 132.8, 132.6, 130.1, 129.0, 128.4, 128.3, 127.3, 124.9, 122.4, 121.6, 93.6 (d, J_{C-F} = 180.1 Hz), 67.8, 60.6, 59.3 (d, J_{C-F} = 22.0 Hz), 38.7 (d, J_{C-F} = 22.1 Hz); ^{19}F NMR (376 MHz, $CDCl_3$): δ −171.49 (m, 1*F*); IR (neat) υ 3296, 1703, 1521, 1264, 1169, 733 cm^{-1}; LCMS (ESI+) m/z = 402.98 $[M + H]^+$; HRMS (ESI) calcd for $C_{25}H_{24}FN_2O_2$ $[M + H]^+$: m/z = 403.1810, found 403.1822.

4.2.6. L-*Ala-Ni-(S)-fluoro-BPB complex (**12**)*

To a solution of **11** (0.11 g, 0.27 mmol) and $Ni(NO_3)_2{\cdot}6H_2O$ (0.16 g, 0.55 mmol) in anhydrous methanol (3 mL) was added a solution of KOH (0.12 mg, 2.20 mmol) and L-alanine (0.12 g, 1.37 mmol) in methanol (2 mL). This mixture was heated at 60 °C with stirring for 24 h—TLC indicated the reaction was complete and the deep red solution concentrated in vacuo before partitioning between water (30 mL) and $CHCl_3$ (20 mL). Trituration of the concentrated organic extract under Et_2O afforded a dark red solid that was isolated by filtration under suction and washed with more Et_2O. The washings were combined and evaporated and triturated again to obtain further material, which was analytically pure without further purification (0.10 mg, 71%).mp 296–298 °C; $[\alpha]_D^{24} + 241$ (c = 1.0, $CHCl_3$); ^{1}H NMR (400 MHz, $CDCl_3$): δ 8.28–8.22 (m, 2*H*, Ar), 8.03 (dd, J = 8.7, 1.1 Hz, 1*H*, Ar), 7.55–7.47 (m, 2*H*, Ar), 7.47–7.41 (m, 1*H*, Ar), 7.38 (t, J = 7.7 Hz, 2*H*, Ar), 7.30–7.17 (m, 2*H*, Ar), 7.12 (ddd, J = 8.7, 6.8, 1.9 Hz, 1*H*, Ar), 6.96–6.90 (m, 1*H*, Ar), 6.70–6.59 (m, 2*H*, Ar), 5.68 (dm, J = 55.1 Hz, 1*H*, CHF), 4.42 (d, J = 12.4 Hz, 1*H*, benzyl CH), 4.25 (ddd, J = 32.8, 14.4, 4.3 Hz, 1*H*, CH), 3.95–3.81 (m, 2*H*, CH), 3.65 (d, J = 12.4 Hz, 1*H*, benzyl CH), 3.32 (dddd, J = 35.7, 15.1, 10.9, 4.5 Hz, 1*H*, CH), 2.94 (m, 2*H*, CH), 1.54 (d, J = 7.0 Hz, 3*H*, CH_3); ^{13}C NMR (101 MHz, $CDCl_3$): δ 180.4, 178.9, 170.8, 142.0, 133.5, 133.4, 133.3, 132.4, 131.8, 129.9, 129.4, 129.1, 129.0, 127.6, 127.3, 126.4, 123.8, 121.1, 91.4 (d, J_{C-F} = 178.6 Hz), 70.1, 66.5, 65.5, 64.0 (d, J_{C-F} = 21.7 Hz), 39.4 (d, J_{C-F} = 21.6 Hz), 21.8; ^{19}F NMR (376 MHz, $CDCl_3$) δ −173.86 (m, 1F); LCMS (ESI+) m/z = 530.06 $[M + H]^+$; HRMS (ESI) calcd for $C_{28}H_{27}FN_3O_3Ni$ $[M + H]^+$: m/z = 530.1385, found 530.1390.

5. X-ray crystal structure determination and structural analysis

The X-ray single crystal data have been collected on a Bruker SMART CCD 6000 (compound **8**, sealed fine-focus tube, graphite monochromator, λMo *K*α, λ = 0.71073 Å) and D8Venture (compounds **1** and **12**, IμS-microsource, focusing mirrors, Photon 100 CMOS detector, λCu *K*α, λ = 1.54178 Å and λMo *K*α, λ = 0.71073 Å, respectively) diffractometers equipped with the Cryostream (Oxford Cryosystems) open-flow nitrogen cryostats at the temperature 120.0(2) K. All structures were solved by direct method and refined by full-matrix least squares on F2 for all data using Olex2 [15] and SHELXTL [26] software. All non-disordered non-hydrogen atoms were refined anisotropically, hydrogen atoms in structure **8** were refined isotropically. The atoms of disordered groups in structure **1** were refined with fixed SOF values in isotropic approximation. The hydrogen atoms in these groups and in the structures **1** and **12** were placed in the calculated positions and refined in riding mode. Crystallographic data for the structures has been deposited with the Cambridge Crystallographic Data Centre as supplementary publication CCDC 1052145–1052147.

Crystal data for **1**: $C_{28}H_{27}N_3NiO_3 \times C_4H_8O$ (M = 584.34), orthorhombic, space group $P2_12_12_1$, a = 9.0963(2), b = 12.1090(3), c = 26.0025(6) Å, V = 2864.10(12) $Å^3$, Z = 4, μ(Cu *K*α) = 1.312 mm^{-1}, D_{calc} = 1.355 g/mm^3, 21,312 reflections measured, 5425 unique (R_{int} = 0.0260) were used in all calculations. The final R_1 was 0.0470 ($5218 > 2\sigma(I)$) and wR_2 was 0.1297 (all data), S = 1.051.

Crystal data for **8**: $C_{28}H_{26}N_3O_3FNi$ (M = 530.23): orthorhombic, space group $P2_12_12_1$, a = 9.4749(5), b = 11.3449(7), c = 44.685(3) Å, V = 4803.2(5) $Å^3$, Z = 8, μ(Mo *K*α) = 0.852 mm^{-1}, D_{calc} = 1.466 g/mm^3,

78,710 reflections measured, 12,765 unique (R_{int} = 0.0738) were used in all calculations. The final R_1 was 0.0364 (10,213 > 2σ(I)) and wR_2 was 0.0766 (all data), S = 0.978.

Crystal data for **12**: $C_{28}H_{26}N_3O_3FNi$ (M = 530.23): orthorhombic, space group $P2_12_12_1$, a = 9.6711(8), b = 10.0617(8), c = 24.6671(19) Å, V = 2400.3(3) Å^3, Z = 4, μ(Mo $K\alpha$) = 0.853 mm^{-1}, D_{calc} = 1.467 g/cm^3, 33,745 reflections measured, 6370 unique (R_{int} = 0.0834) which were used in all calculations. The final R_1 was 0.0584 (5748 > 2σ(I)) and wR_2 was 0.1369 (all data), S = 1.077.

These data can be viewed free of charge via http://www.ccdc.cam.ac.uk/cont/retrieving.html or from the CCDC, 12 Union Road, Cambridge CB2 1EZ, UK; fax: +44 1223 336033 E-mail: deposit@ccdc.cam.ac.uk.

Acknowledgements

This work was supported by Durham University and the Cambridge Crystallographic Data Centre (NJT) and the Engineering and Physical Sciences Research Council (CRC) [EP/J015989/1]. Dr. Ehmke Pohl (Chemistry Department, Durham University) is thanked for his support and helpful suggestions relating to the analysis of the X-ray crystal structures obtained. Dr. Martin Walker (Chemistry Department, Durham University) is thanked for technical assistance in performing the DFT calculations.

References

[1] (a) J. Wang, M. Sanchez-Rosello, J.L. Aceña, C. del Pozo, A.E. Sorochinsky, S. Fustero, V.A. Soloshonok, H. Liu, Chem. Rev. 114 (2013) 2432–2506;
(b) D. O'Hagan, J. Fluor. Chem. 131 (2010) 1071–1081;
(c) S. Purser, P.R. Moore, S. Swallow, V. Gouverneur, Chem. Soc. Rev. 37 (2008) 320–330;
(d) I. Ojima, J. Org. Chem. 78 (2013) 6358–6383;
(e) R. Filler, R. Saha, Future Med. Chem. 1 (2009) 777–791.
[2] D.Y. Buissonneaud, T. van Mourik, D. O'Hagan, Tetrahedron 66 (2010) 2196–2202.
[3] D. Cahard, V. Bizet, Chem. Soc. Rev. 43 (2014) 135–147.
[4] C. Sparr, E. Salamanova, W.B. Schweizer, H.M. Senn, R. Gilmour, Chem. Eur. J. 17 (2011) 8850–8857.
[5] P.W. Chia, M.R. Livesey, A.M.Z. Slawin, T. van Mourik, D.J.A. Wyllie, D. O'Hagan, Chem. Eur. J. 18 (2012) 8813–8819.
[6] J.A. Hodges, R.T. Raines, J. Am. Chem. Soc. 127 (2005) 15923–15932.
[7] (a) C. Sparr, W.B. Schweizer, H.M. Senn, R. Gilmour, Angew. Chem. Int. Ed. 48 (2009) 3065–3068, For examples see:;
(b) C. Sparr, E.-M. Tanzer, J. Bachmann, R. Gilmour, Synthesis 8 (2010) 1394–1397;
(c) C. Sparr, R. Gilmour, Angew. Chem. 122 (2010) 6670–6673;
(d) C. Sparr, L.E. Zimmer, R. Gilmour, in: S. Bräse, M. Christmann (Eds.), Asymmetric Syntheses. More Methods and Applications, Wiley-VCH Verlag GmbH & Co., Weinheim, 2011, pp. 117–124;
(e) E.-M. Tanzer, R. Gilmour, Chem. Eur. J. 18 (2012) 2006;
(f) E.-M. Tanzer, L.E. Zimmer, W.B. Schweizer, R. Gilmour, Chem. Eur. J. 18 (2012) 11334;
(g) Y.P. Rey, R. Gilmour, J. Org. Chem. 9 (2013) 2812–2820;
(h) I.G. Molnar, E.-M. Tanzer, C. Daniliuc, R. Gilmour, Chem. Eur. J. 20 (2014) 794–800;
(i) Y.P. Rey, L.E. Zimmer, C. Sparr, E.-M. Tanzer, W.B. Schweizer, H.M. Senn, S. Lakhdar, R. Gilmour, Eur. J. Org. Chem. 2014 (2014) 1202–1211.
[8] (a) A.E. Sorochinsky, J.L. Aceña, H. Moriwaki, T. Sato, V.A. Soloshonok, Amino Acids 45 (2013) 691–718;
(b) A.E. Sorochinsky, J.L. Aceña, H. Moriwaki, T. Sato, V.A. Soloshonok, Amino Acids 45 (2013) 1017–1033;
(c) J.L. Aceña, A.E. Sorochinsky, V. Soloshonok, Amino Acids 46 (2014) 2047–2073;
(d) J.L. Aceña, A.E. Sorochinsky, H. Moriwaki, T. Sato, V.A. Soloshonok, J. Fluorine Chem. 155 (2013) 21–38;
(e) Y.N. Belokon, Y.E. Zeltzer, V.I. Bakhmutov, M.B. Saporovskaya, M.G. Ryzhov, A.I. Yanovsky, Y.T. Struchkov, V.M. Belikov, J. Am. Chem. Soc. 105 (1983) 2010–2017;
(f) Y.N. Belokon, A.G. Bulychev, S.V. Vitt, Y.T. Struchkov, A.S. Batsanov, T.V. Timofeeva, V.A. Tsyryapkin, M.C. Ryzhov, L.A. Lysova, V.I. Bakhmutov, V.M. Belikov, J. Am. Chem. Soc. 107 (1985) 4252–4259.
[9] H. Moriwaki, D. Resch, H. Li, I. Ojima, R. Takeda, J.L. Aceña, V.A. Soloshonok, Beilstein J. Org. Chem. 10 (2014) 442–448.
[10] M. Bergagnini, K. Fukushi, J. Han, N. Shibata, C. Roussel, T.K. Ellis, J.L. Aceña, V.A. Soloshonok, Org. Biomol. Chem. 12 (2014) 1278–1291.
[11] N.H. Campbell, D.L. Smith, A.P. Reszka, S. Neidle, D. O'Hagan, Org. Biomol. Chem. 9 (2011) 1328–1331.
[12] H. Ueki, T.K. Ellis, C.H. Martin, T.U. Boettiger, S.B. Bolene, V.A. Soloshonok, J. Org. Chem. 68 (2003) 7104–7107.
[13] Y.N. Belokon, V.I. Tararov, V.I. Maleev, T.F. Savel'eva, M.G. Ryzhov, Tetrahedron: Asymmetry 9 (23) (1998) 4249–4252.
[14] (a) Y.W. Kim, T.N. Grossmann, G.L. Verdine, Nat. Protoc. 6 (2011) 761–771;
(b) G.H. Bird, W.C. Crannell, L.D. Walensky, Curr. Protoc. Chem. Biol. 3 (2011) 99–117;
(c) W. Qiu, V.A. Soloshonok, C. Cai, X. Tang, V.J. Hruby, Tetrahedron 56 (2000) 2577–2582;
(d) Y.N. Belokon, N.I. Chernoglazova, C.A. Kochetkov, N.S. Garbalinskaya, V.M. Belikov, J. Chem. Soc., Chem. Commun. 3 (1985) 171–172.
[15] O.V. Dolomanov, L.J. Bourhis, R.J. Gildea, J.A.K. Howard, H. Puschmann, J. Appl. Crystallogr. 42 (2009) 339–341.
[16] Hermes—Accessed on web (08/04/2014) at ⟨http://www.ccdc.cam.ac.uk/Solutions/GoldSuite/pages/GoldSuite.aspx⟩.
[17] Q. Jing, H. Li, L.J. Roman, P. Martásek, T.L. Poulos, R.B. Silverman, ACS Med. Chem. Lett. 5 (2014) 56–60.
[18] W. Zhuang, X. Zhao, G. Zhao, L. Guo, Y. Lian, J. Zhou, D. Fang, Bioorg. Med. Chem. 17 (2009) 6540–6546.
[19] B.R. Kim, H.G. Lee, S.B. Kang, G.H. Sung, J.J. Kim, J.K. Park, Y.J. Yoon, Synthesis 44 (2012) 42–50.
[20] Y.Q. Tang, J.M. Lu, X.R. Wang, L.X. Shao, Tetrahedron 66 (2010) 7970–7974.
[21] H. Ueki, T.K. Ellis, C.H. Martin, T.U. Boettiger, S.B. Bolene, V.A.J. Soloshonok, J. Org. Chem. 68 (2003) 7104–7107.
[22] J.A.K. Howard, V.J. Hoy, D. O'Hagan, G.T. Smith, Tetrahedron 52 (1996) 12613.
[23] V.R. Thalladi, H.-C. Weiss, D. Bläser, R. Boese, A. Nangia, G.R. Desiraju, J. Am. Chem. Soc. 120 (1998) 8702–8710.
[24] H.-C. Weiss, R. Boese, H.L. Smith, M.M. Haley, Chem. Commun. 24 (1997) 2403–2404.
[25] A. Cochi, D. Gomez Pardo, J. Cossy, Org. Lett. 13 (2011) 4442–4445.
[26] G.M. Sheldrick, Acta Crystallogr. A64 (2008) 112–122.